Review

Scale Effects on the Hydrodynamics of Bubble Columns Operating in the Homogeneous Flow Regime

By *R. Krishna*, *J. M. van Baten*, and *M. I. Urseanu**

Measurements of gas holdup were made with the air-water system in bubble columns of 0.1, 0.15 and 0.38 m diameter, equipped with identical distribution devices. For operation with superficial gas velocity in the range 0–0.04 m/s, the total gas holdup was found to decrease with increasing column diameter. Of all the literature correlations for the gas holdup, only the Zehner correlation anticipates this decrease in the gas holdup with increasing column diameter. The reason for this scale dependence is because the strength of the liquid circulations increases with increasing scale. Such circulations accelerate the bubbles travelling upwards in the central core. Computational fluid dynamics (CFD) simulations were carried out using the Eulerian description for both the gas and the liquid phases in order to verify the scale dependence of the hydrodynamics. Interactions between the bubbles and the liquid are taken into account in terms of a momentum exchange, or drag, coefficient. The drag coefficient is determined from the Mendelson correlation for bubble rise velocity. The turbulence in the liquid phase is described using the k-ε model. The simulation results verify the trends predicted by the Zehner (1989) correlation. It is concluded that Eulerian simulations are useful tools for scaling up bubble columns.

1 Introduction

Bubble columns are widely used in industry for carrying out gas-liquid reactions. They are simple in construction and particularly suited for carrying out relatively slow chemical reactions requiring large liquid holdups in the reactor. Often, the superficial gas velocity is restricted to values lower than say 0.04 m/s and the bubble column operates in the homogeneous flow regime [1], the focus of attention in this paper. The overall rate of chemical reaction is governed by the liquid holdup and this parameter has to be predicted with good accuracy. There are several correlations in the literature for estimating the gas holdup as a function of the superficial gas velocity and system properties. Fig. 1 (a) presents the results of the calculation of the gas holdup for the air-water system as function of the superficial gas velocity U in the range 0–0.04 m/s for a column of diameter D_T = 0.38 m, using a selection of literature correlations [2–7]. We see that there is a wide spread in the estimation of the gas holdup. Fig. 1 (b) presents the results of the calculation of the gas holdup for the air-water system taking U = 0.02 m/s and varying the column diameter D_T.

The Zehner [7] correlation deserves special mention because it is the only literature correlation that anticipates a significant decrease in the gas holdup with increasing column diameter. All other correlations do not anticipate any dependence of the gas holdup on the column diameter. Let us examine the reasons behind the scale dependence of the gas holdup predicted by the Zehner correlation[1]:

$$\varepsilon = \frac{U/\alpha}{\sqrt{1+4\left(\frac{U}{\alpha}\right)^{2/3}\frac{V_L(0)}{\alpha}}} \tag{1}$$

The parameter α in Eq. (1) is dependent on the system properties and is given by:

$$\alpha = 1.4\left(\frac{\sigma}{\rho_L}\frac{\rho_L-\rho_G}{\rho_L}g\right)^{1/4} \tag{2}$$

The parameter $V_L(0)$ in Eq. (1) represents the velocity of the liquid at the center of the column and is a measure of the strength of the liquid circulations; this is correlated by Zehner [7] by:

$$V_L(0) = \left(\frac{1}{2.5}\frac{\rho_L-\rho_G}{\rho_L}\ U\ gD_T\right)^{1/2} \tag{3}$$

Liquid circulations increase with increasing column diameter and this is the reason that the gas holdup, calculated using Eq. (1), shows a decreasing trend with increasing D_T.

The main objective of our paper is to verify the scale dependence of the gas holdup and to suggest a scale-up strategy for commercial scale reactors. We carried out experiments in columns of 0.1, 0.15 and 0.38 m in diameter with the air-water system to study the scale dependence of the gas holdup.

Several recent publications have established the potential of computational fluid dynamics (CFD) for describing the hydrodynamics of bubble columns [8–24], with some degree of success in describing scale effects. We resort to CFD simulations for understanding the scale dependence of the hydrodynamics of bubble columns operating in the homogeneous bubbly flow regime.

[*] R. Krishna (author to whom correspondence should be addressed), J. M. van Baten, M. I. Urseanu, Department of Chemical Engineering, University of Amsterdam, Nieuwe Achtergracht 166, 1018 WV Amsterdam, The Netherlands; e-mail: krishna@its.chem.uva.nl)

1) List of symbols at the end of the paper.

  0930-7516/01/0505-0451 $ 17.50+.50/0

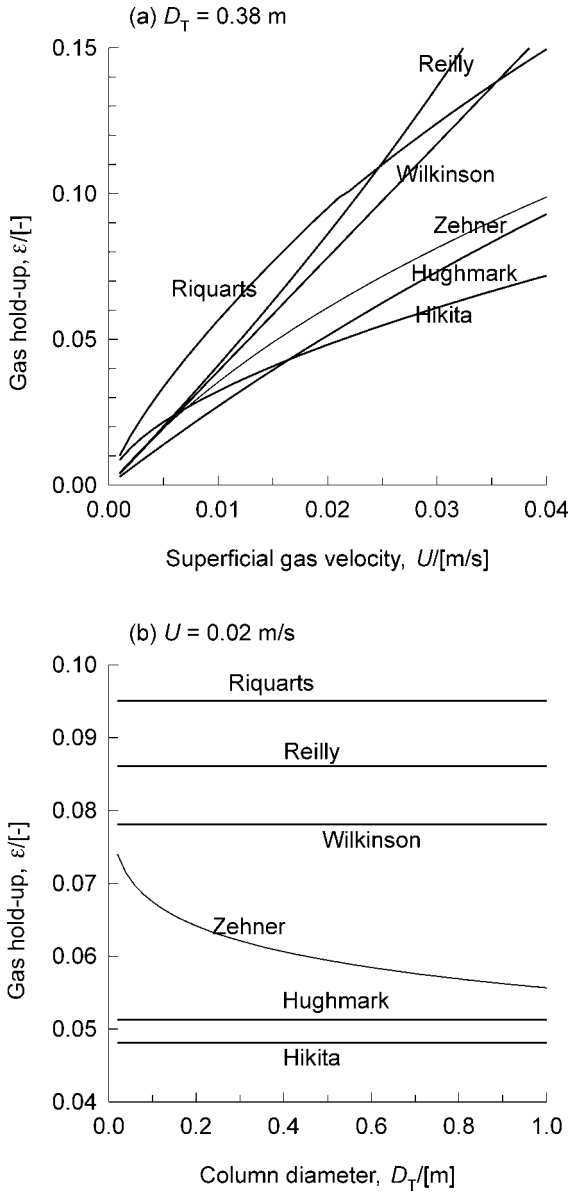

Figure 1. (a) Gas holdup as a function of the superficial gas velocity U for a column of diameter D_T = 0.38 m. (b) Gas holdup as a function of column diameter D_T for a superficial gas velocity U = 0.02 m/s. The calculations were carried out using a selection of literature correlations [2–7].

2 Experimental

Experiments were carried out in columns of 0.1, 0.15 and 0.38 m in diameter. Air was used as the gas phase. The liquid phase used in the experiments consisted of demineralized water. In all the experiments the initial liquid height was kept constant at 1 m. A typical column configuration for the 0.15 m diameter column is shown in Fig. 2. All columns were fitted with similar sieve plate distributors with 0.5 mm diameter holes on a triangular pitch of 7 mm. In the 0.15 m diameter column, for example, a total of 625 holes were drilled. The total gas holdup was determined by measuring the hydrostatic pressure using a Validyne pressure sensor.

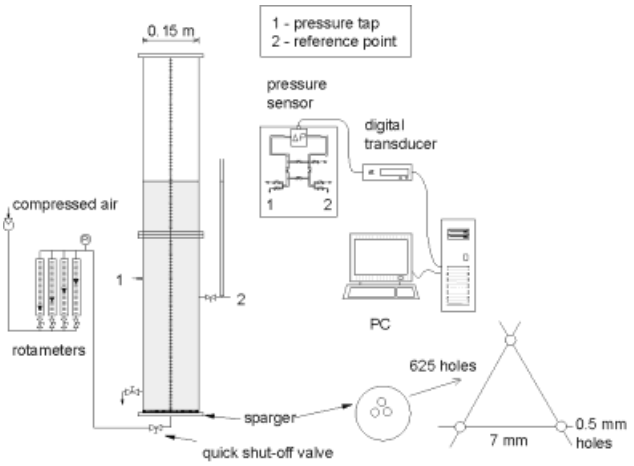

Figure 2. Typical experimental setup for column of diameter 0.15 m.

3 CFD Simulations for Homogeneous Bubbly Flow Regime

For the homogeneous regime of operation of bubble columns a more or less uniform bubble size is obtained. For the air-water system the bubbles are in the size range of 1–6 mm and are either spherical or ellipsoidal in shape depending on the physical properties of the liquid [25,26].

For either gas or liquid phase the volume-averaged mass and momentum conservation equations in the Eulerian framework are given by

$$\frac{\partial(\varepsilon_k \rho_k)}{\partial t} + \nabla \cdot (\rho_k \varepsilon_k \mathbf{u}_k) = 0 \tag{4}$$

$$\frac{\partial(\rho_k \varepsilon_k \mathbf{u}_k)}{\partial t} + \nabla \cdot \left(\rho_k \varepsilon_k \mathbf{u}_k \mathbf{u}_k - \mu_k \varepsilon_k \left(\nabla \mathbf{u}_k + (\nabla \mathbf{u}_k)^T\right)\right) = -\varepsilon_k \nabla p + \mathbf{M}_{kl} + \rho_k \mathbf{g} \tag{5}$$

where ρ_k, $\mathbf{u}_k$, ε_k and μ_k represent, respectively, the macroscopic density, velocity, volume fraction and viscosity of the kth phase, p is the pressure, $\mathbf{M}_{kl}$, the interphase momentum exchange between phase k and phase l and $\mathbf{g}$ is the gravitational acceleration.

The momentum exchange between the gas (bubble) phase (subscript b) and liquid phase (subscript L) phases is given by:

$$\mathbf{M}_{L,b} = \frac{3}{4}\rho_L \frac{\varepsilon_b}{d_b} C_D (\mathbf{u}_b - \mathbf{u}_L)|\mathbf{u}_b - \mathbf{u}_L| \tag{6}$$

The interphase drag coefficient is calculated from equation

$$C_D = \frac{4}{3}\frac{\rho_L - \rho_G}{\rho_L}\mathbf{g} d_b \frac{1}{V_{b,0}^2} \tag{7}$$

where $V_{b,0}$ is the rise velocity of a single bubble. We have only included the drag force contribution to $\mathbf{M}_{L,b}$, in keeping with the works of Sanyal *et al.* [22] and Sokolichin and Eigenberger [24]. The added mass, Magnus and and lift force contributions were all ignored in the present analysis.

For the continuous, liquid, phase, the turbulent contribution to the stress tensor is evaluated by means of the k-ε model, using standard single phase parameters $C_\mu = 0.09$, $C_{1\varepsilon} = 1.44$, $C_{2\varepsilon} = 1.92$, $\sigma_k = 1$ and $\sigma_\varepsilon = 1.3$. The applicability of the k-ε model has been considered in detail by Sokolichin and Eigenberger [24]. No turbulence model is used for calculating the velocity fields inside the dispersed bubble phase.

From visual observations of bubble column operations with the air-water system, the small bubbles were observed to be in the 3–6 mm size range. The rise velocity of air bubbles is practically independent of the bubble diameter in this size range and the Mendelson [27] equation for the rise velocity

$$V_{b,0} = \sqrt{2\sigma/\rho_L d_b + \mathbf{g} d_b/2} \tag{8}$$

is used in the simulation model developed here, taking the bubble size to be 0.004 m. Fig. 3 compares experimental data of Krishna *et al.* [14] on the rise velocity of single gas bubbles in the 2–10 mm range with the Mendelson [27] and Harmathy [28] correlations. It is seen that Eq. (8) provides a good representation of the experimental data.

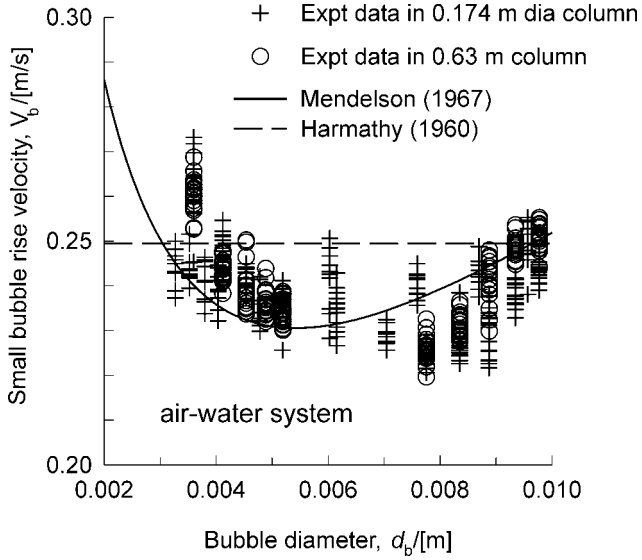

Figure 3. Small bubble rise velocity in air-water system. Experimental data of Krishna *et al.* [14] compared with the Mendelson [27] and Harmathy [28] correlations.

A commercial CFD package CFX 4.3 of AEA Technology, Harwell, UK, was used to solve the equations of continuity and momentum. This package is a finite volume solver, using body-fitted grids. The grids are nonstaggered and all variables are evaluated at the cell centers. An improved version of the Rhie-Chow [29] algorithm is used to calculate the velocity at the cell faces. The pressure-velocity coupling is obtained using the SIMPLEC algorithm [30]. For the convective terms in Eqs. (4) and (5) hybrid differencing was used. A fully implicit backward differencing scheme was used for the time integration.

Simulations were carried out for columns of 0.1, 0.15 and 0.38 m in diameter with the air-water system operating at superficial gas velocities U = 0.01, 0.02 and 0.025 m/s. All simulations were carried out using cylindrical axisymmetry with the grid specified in Fig. 4.

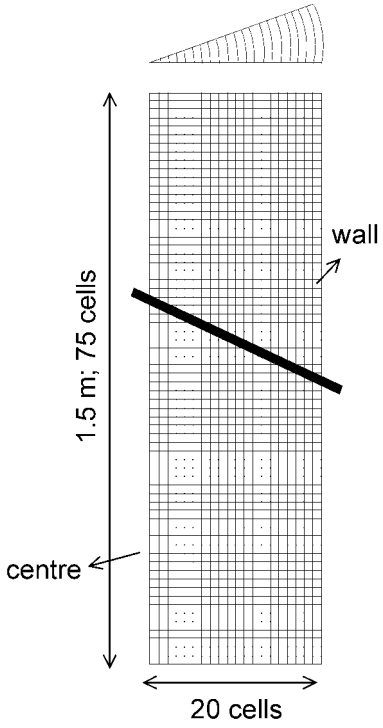

Figure 4. Grid used in the 2-D cylindrical axisymmetric simulations.

The total column height was taken to be 1.5 m. The number of grid cells in the radial and axial directions were 20 and 75 respectively, making a total of 1500 cells. In all the simulations the column was first filled with water to a height of 1 m and at time t = 0, air was introduced at the specified superficial velocity, U, at the bottom of the column. The air was injected at the innermost 17 of 20 grid cells to prevent a circulation in which the liquid flows up near the wall and travels down the core. A pressure boundary condition was applied to the top of the column. A standard no-slip boundary condition was applied at the wall. The time-stepping strategy used in the transient simulations for attainment of steady state was typically: 50 steps at 1×10^{-5} s, 100 steps at 2×10^{-5} s, 100 steps at 5×10^{-5} s, 100 steps at 1×10^{-4} s, 100 steps at 2×10^{-4} s, 100 steps at 5×10^{-4} s, 100 steps at 1×10^{-3} s, 200 steps at 3×10^{-3} s, 2150 steps at 5×10^{-3} s, 7000 steps at 1×10^{-2} s. The simulations were carried out on a Silicon Graphics Power Indigo workstation with an R8000 processor. Each simulation was completed in about 2 days. Typical transient development of the velocities of the liquid, small and large bubbles at a position 0.7 m above the distributor are shown in Fig. 5 (a) for $U = 0.02$ m/s and $D_T = 0.38$ m. When steady state is established, the cumulative gas holdup can be determined along the column height. A typical profile of the cumulative gas holdup is shown in Fig. 5 (b). All the gas holdup data reported in this paper correspond to the cumulative gas holdup at a height of 0.7 m above the distributor.

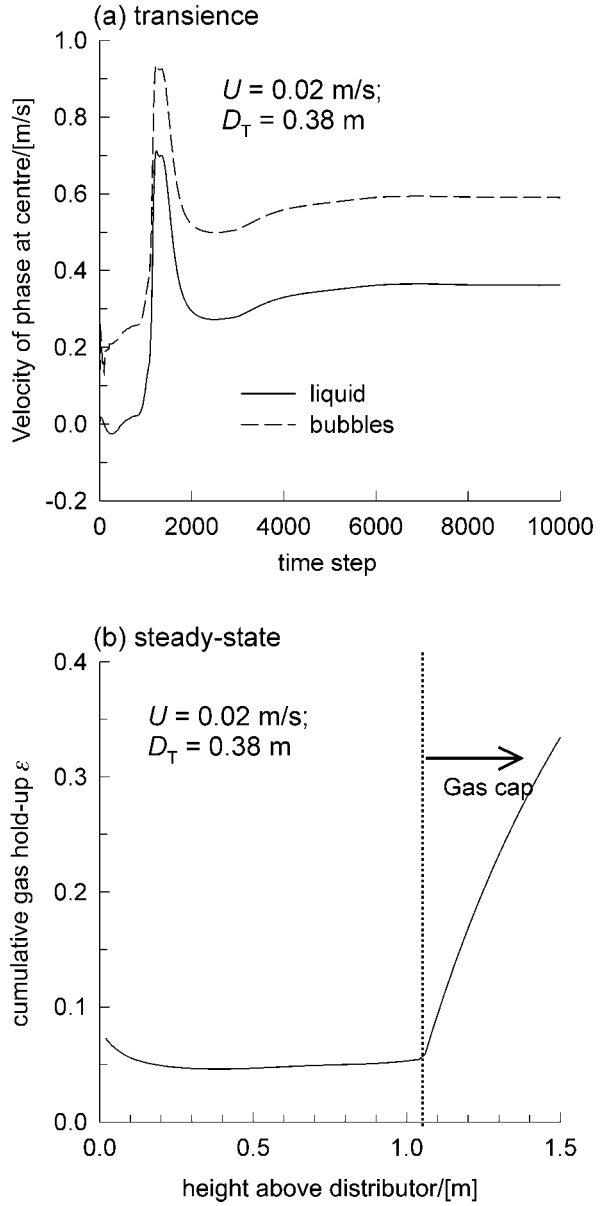

Figure 5. (a) Transient velocity monitored at height 0.7 m above distributor $U = 0.02$ m/s, $D_T = 0.38$ m. (b) Cumulative gas holdup at steady state.

Further details of the simulations, including animations of column start-up dynamics, are available on our web site: http://ct-cr4.chem.uva.nl/homogeneous/.

4 Results and Discussion

Both experimental data (Fig. 6) and CFD simulations (Fig. 7) confirm the trends predicted by the Zehner [7] correlation (Eq. 1) concerning the influence of the column diameter on the gas holdup. Fig. 7 compares the CFD simulations with the predictions of the Zehner correlation; the agreement between the two approaches can be considered to be remarkably good. When comparing the experimental data with the CFD simulations, we note that though the simulations predict the right trends, the gas holdup values are somewhat lower in magnitude. The reason for this discrepancy is to be found in the particular drag relations, Eqs. (7) and (8), along with the choice of bubble diameter (0.004 m). With proper tuning of these parameters, an improved match can be obtained between experiment and simulations.

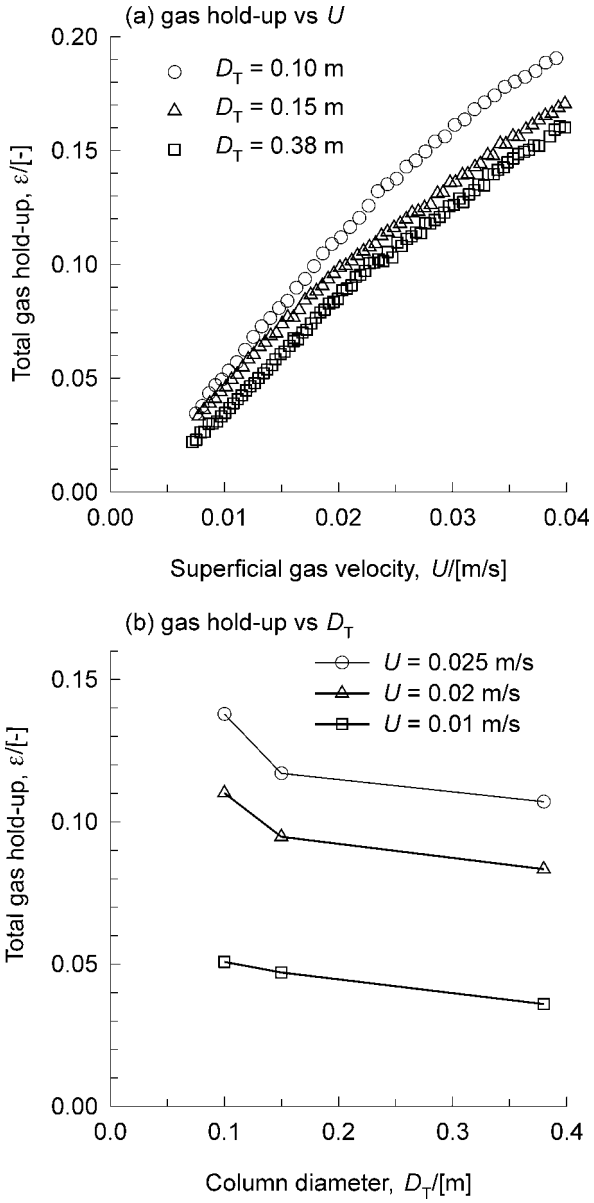

Figure 6. (a) Experimental data on gas holdup as a function of the superficial gas velocity U for columns of diameter $D_T = 0.1, 0.15$ and 0.38 m. (b) Gas holdup as a function of column diameter D_T for a superficial gas velocity $U = 0.01, 0.02$, and 0.025 m/s.

The major advantage of the CFD approach is that besides the total gas holdup, complete information is obtained on the hydrodynamics of bubble columns. The radial distribution of the liquid velocity, $V_L(r)$, obtained from CFD simulations are shown in Figs. 8 (a) and (b). The downflow of the liquid phase near the wall region is evident. If the radial liquid velocity distributions $V_L(r)$ are normalized with respect to the center-

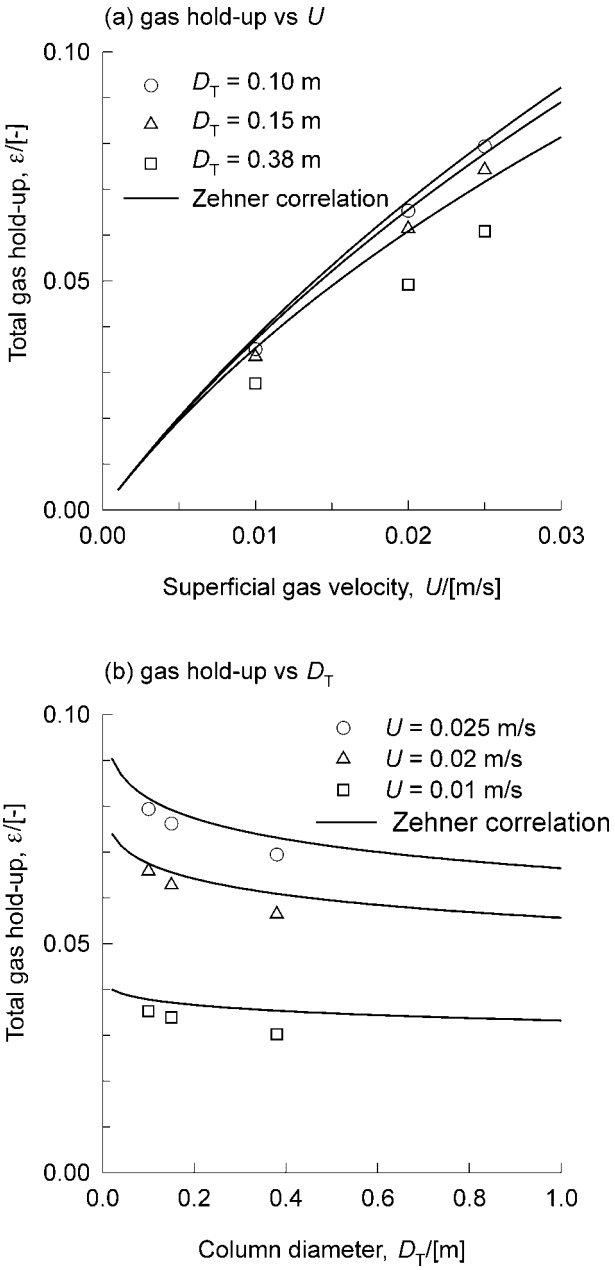

Figure 7. (a) CFD simulation data on gas holdup as a function of the superficial gas velocity U for columns of diameter D_T = 0.1, 0.15 and 0.38 m. (b) Gas holdup as a function of column diameter D_T for superficial gas velocities U = 0.01, 0.02, and 0.025 m/s. The continuous lines are drawn using the Zehner correlation, Eq. (1).

line liquid velocity $V_L(0)$, we see that the profiles for all simulations are almost identical, see Fig. 9. This implies that the magnitude of the liquid circulations can be characterized by a single parameter, the center-line velocity $V_L(0)$. This center-line liquid velocity increases with increasing U and with increasing D_T, see Fig. 10. Fig. 10 also compares the CFD simulation values of $V_L(0)$ with the estimations using Eq. (3) of Zehner [7]. The liquid flowing upwards in the central core of the column has the effect of accelerating the bubbles. The downflowing liquid in the wall region tends to drag the bubbles downwards. The CFD simulations of the radial distribution of the bubble velocities, $V_b(r)$, shown in Figs. 11 (a) and (b), verify these effects. Note that near the wall the bubbles can even travel downwards; this was also observed visually in the experiments.

From the radial distribution of bubble velocities the cross-sectional area average bubble rise velocity, V_b, can be calculated. This average bubble rise velocity is found to increase with increase column diameter, see Fig. 12. Even though the single bubble rise velocity, $V_{b,0}$, is independent of the column diameter (cf. Eq. (8)), the effective bubble swarm velocity is scale-dependent.

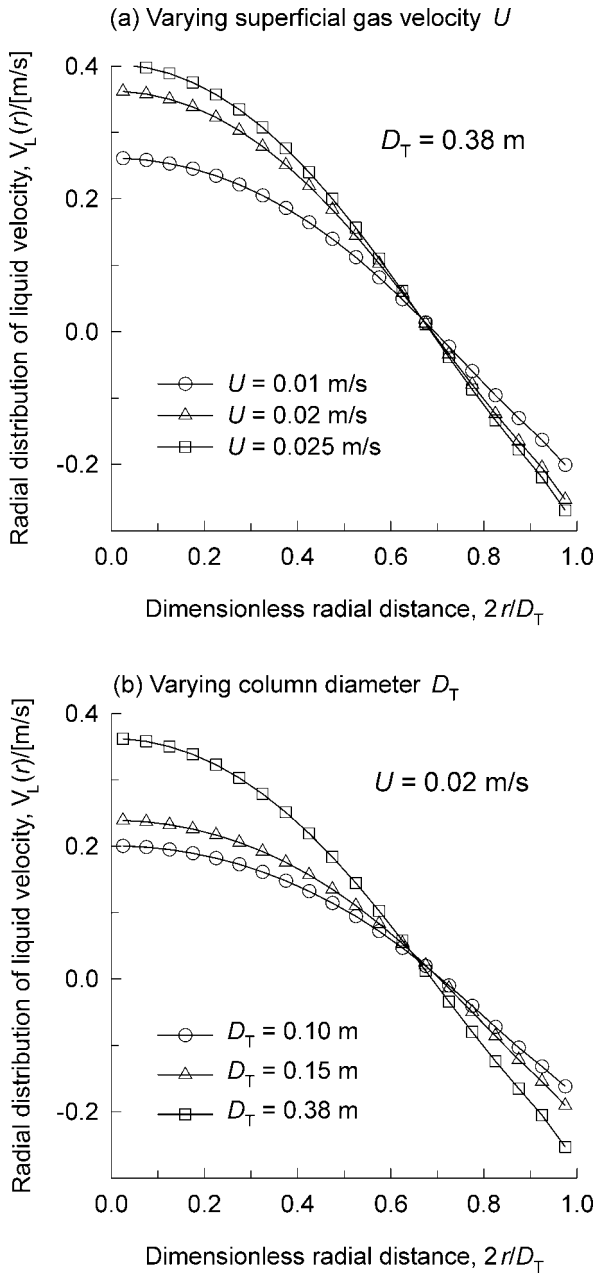

Figure 8. (a) Radial distribution of liquid velocity $V_L(r)$ for a column of diameter D_T = 0.38 m and varying superficial gas velocities U = 0.01, 0.02, and 0.025 m/s. (b) Radial distribution of liquid velocity $V_L(r)$ for superficial gas velocity U = 0.02 m/s and varying column diameters D_T = 0.1, 0.15 and 0.38 m.

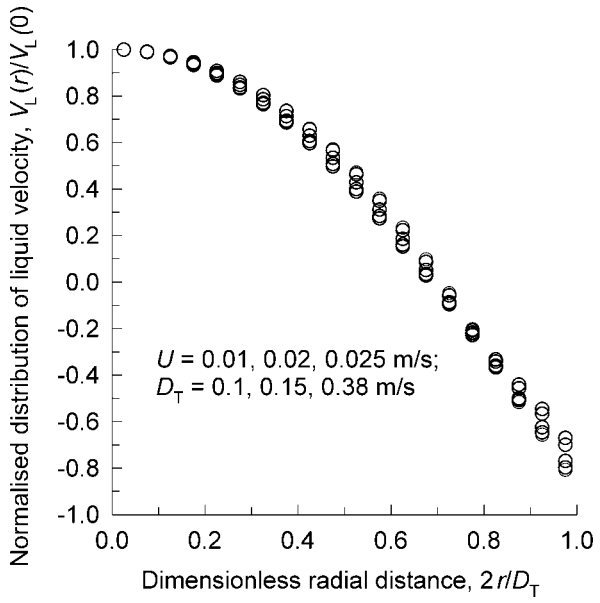

Figure 9. Normalized distribution of liquid velocity, $V_L(r)/V_L(0)$ for columns of diameter D_T = 0.1, 0.15 and 0.38 m operating at superficial gas velocities U = 0.01, 0.02, and 0.025 m/s.

5 Conclusions

From the experimental work and CFD simulations the following conclusions can be drawn:

1. The gas holdup in a bubble column operating in the homogeneous flow regime decreases with increasing column diameter. This decrease in the gas holdup is caused by the increasing liquid circulations with increasing column diameter.
2. The trends in the CFD simulations agree with the predictions of the Zehner [7] correlation for the center-line velocity $V_L(0)$ and the gas holdup.

We recommend the use of CFD simulations for scale-up purposes.

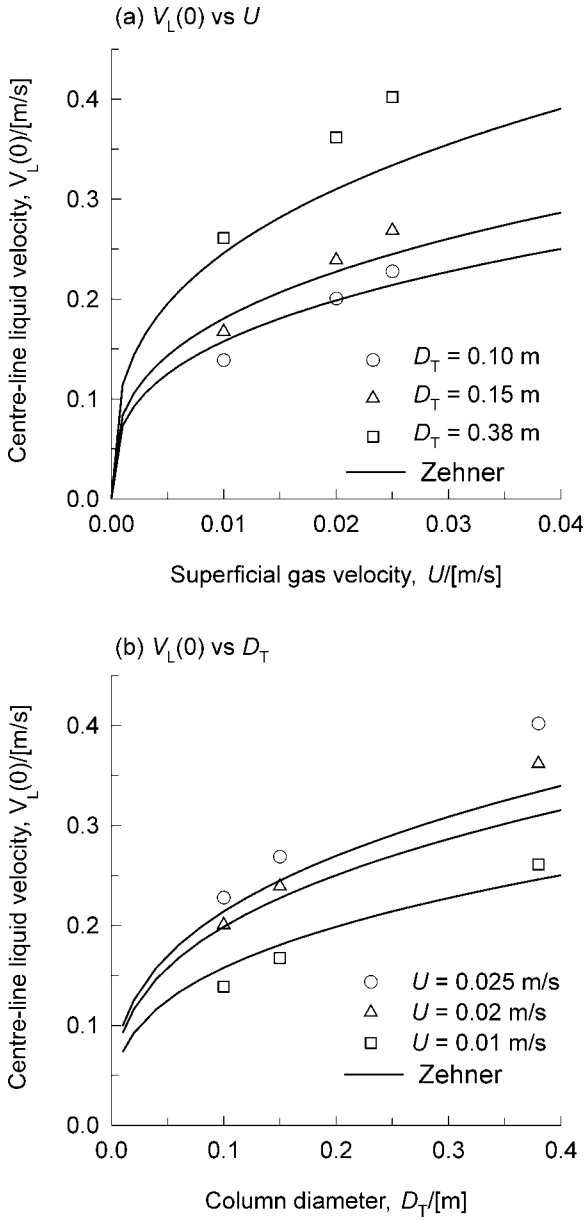

Figure 10. (a) CFD simulation data on center-line velocity $V_L(0)$ as a function of the superficial gas velocity U for columns of diameter D_T = 0.1, 0.15 and 0.38 m. (b) CFD simulation data on center-line velocity $V_L(0)$ as a function of column diameter D_T for superficial gas velocities U = 0.01, 0.02, and 0.025 m/s. The continuous lines are drawn using the Zehner correlation, Eq. (3).

Acknowledgement

The Netherlands Organisation for Scientific Research (NWO) is gratefully acknowledged for providing financial assistance in the form of a "programmasubsidie".

Received: June 30, 2000 [CET 1268]

Symbols used

C_D	[–]	drag coefficient, dimensionless
d_b	[m]	diameter of bubble
D_T	[m]	column diameter
g	[9.81 m s^{-2}]	gravitational acceleration
M	[Nm^{-3}]	interphase momentum exchange term
p	[Pa]	system pressure
r	[m]	radial coordinate
t	[s]	time
u	[m/s]	velocity vector
U	[m s^{-1}]	superficial gas velocity
$V_b(r)$	[m s^{-1}]	radial distribution of bubble velocity
$V_L(r)$	[m s^{-1}]	radial distribution of liquid velocity
V_b	[m s^{-1}]	cross-sectional area average rise velocity of bubble swarm
$V_{b,0}$	[m s^{-1}]	single bubble rise velocity
$V_L(0)$	[m s^{-1}]	center-line liquid velocity

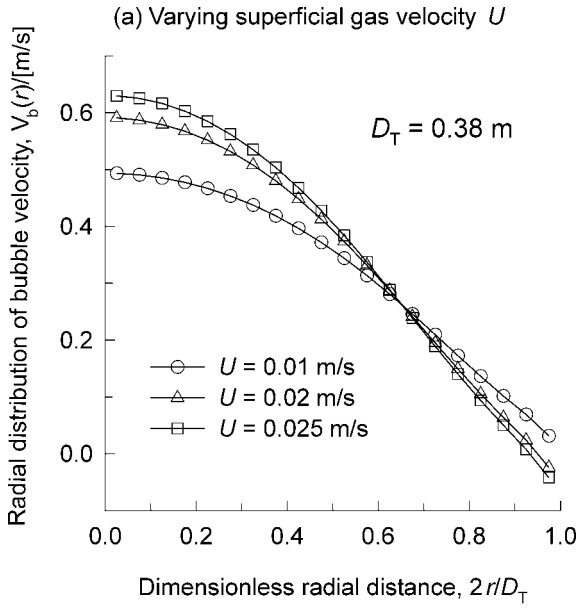

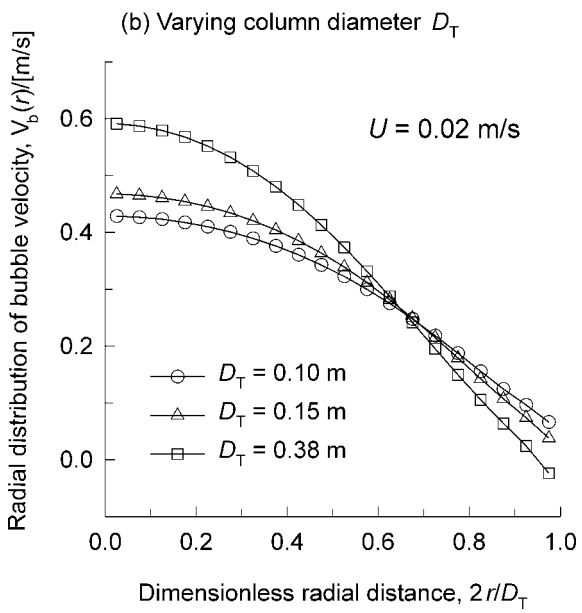

Figure 11. (a) Radial distribution of bubble velocity $V_b(r)$ for a column of diameter D_T = 0.38 m and varying superficial gas velocities U = 0.01, 0.02, and 0.025 m/s. (b) Radial distribution of bubble velocity $V_b(r)$ for superficial gas velocity U = 0.02 m/s and varying column diameters D_T = 0.1, 0.15 and 0.38 m.

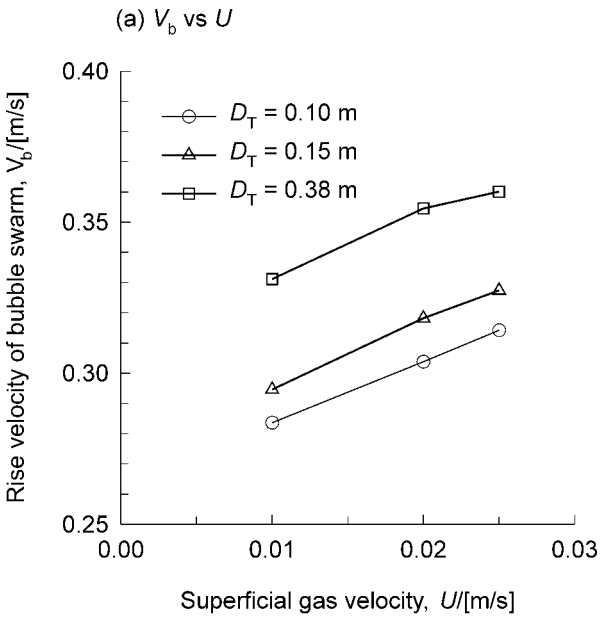

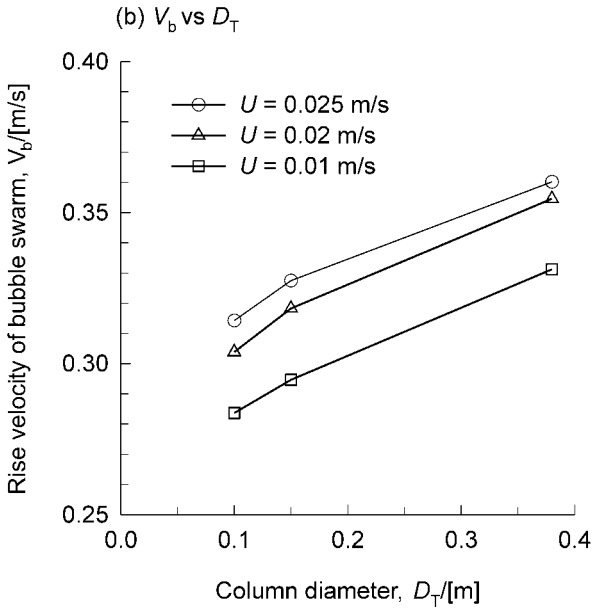

Figure 12. (a) CFD simulation data on cross-sectional averaged rise velocity V_b of bubble swarm as a function of the superficial gas velocity U for columns of diameter D_T = 0.1, 0.15 and 0.38 m. (b) CFD simulation data on cross-sectional averaged bubble rise velocity V_b as a function of column diameter D_T for superficial gas velocities U = 0.01, 0.02, and 0.025 m/s.

Greek symbols

α	[–]	parameter defined by Eq. (2), dimensionless
ε	[–]	total gas holdup, dimensionless
μ_L	[Pa s]	viscosity of liquid phase
ρ	[kg m^{-3}]	density of phase
σ	[N m^{-1}]	surface tension of liquid phase

Subscripts

b	referring to bubbles
G	referring to gas
L	referring to liquid
T	tower or column

References

[1] Deckwer, W. D., *Bubble Column Reactors, John WILEY & Sons, New York 1992.*
[2] Hikita, H.; Asai, S.; Tanigawa, K.; Kitao, M., *Chem. Eng J. 20* (1980) p. 59.
[3] Hughmark, G. A., *Ind. Eng. Chem. Process Des. Dev. 6* (1967) p. 218.
[4] Reilly, I. G.; Scott, D. S.; De Bruijn, T. J. W.; Jain, A. K.; Piskorz, J., *Can. J. Chem. Eng. 64* (1986) p. 705.
[5] Riquarts, H. P.; Pilhofer, T., *Verfahrenstechnik 12* (1978) p. 77.
[6] Wilkinson, P. M.; Spek, A. P.; Van Dierendonck, L. L., *AIChE J. 38 (1992) p. 544.*
[7] Zehner, P., *Dechema-Monogr. 114 (1989) p. 215.*
[8] Grevskott, S.; Sannæs, B. H.; Dudukovic, M. P.; Hjarbo, K. W.; Svendsen, H. F., *Chem. Eng. Sci 51* (1996) p. 1703.
[9] Jakobsen, H. A.; Sannæs, B. H.; Grevskott, S.; Svendsen, H. F., *Ind. Eng. Chem. Res. 36* (1997) p. 4052.
[10] Krishna, R.; van Baten, J. M.; Ellenberger, J., *Powder Technology 100* (1998) p. 137.
[11] Krishna, R.; Urseanu, M. I.; van Baten, J. M.; Ellenberger, J., *Chem. Eng. Sci. 54* (1999) p. 171.
[12] Krishna, R.; van Baten, J. M., *Nature 398* (1999) p. 208.
[13] Krishna, R.; Urseanu, M. I.; van Baten, J. M.; Ellenberger, J., *Chem. Eng. Sci 54* (1999) p. 4903.
[14] Krishna, R.; Urseanu, M. I.; van Baten, J. M.; Ellenberger, J., *Int. Commn. Heat Mass Transf. 26* (1999) p. 781.
[15] Krishna, R.; van Baten, J. M., *Int. Commn. Heat Mass Transf. 26* (1999) p. 965.
[16] Krishna, R.; van Baten, J. M.; Urseanu, M. I., *Chem. Eng. Sci. 55* (2000) p. 3275.
[17] Krishna, R.; van Baten, J. M.; Urseanu, M. I.; Ellenberger, J., *Chem. Eng. Process. 39* (2000) p. 433.
[18] Krishna, R.; Urseanu, M. I.; van Baten, J. M.; Ellenberger, J., *Chem. Eng. J. 78* (2000) p. 43.
[19] Krishna, R., *Oil & Gas Sci. and Technol., Revue de L'Institut Français du Petrole 55* (2000) p. 359.
[20] Lapin, A.; Lübbert, A., *Chem. Eng. Sci. 49* (1994) p. 3661.
[21] Pan, Y.; Dudukovic, M. P.; Chang, M., *AIChE J. 46* (2000) p. 434.
[22] Sanyal, J.; Vasquez, S.; Roy, S.; Dudukovic, M. P., *Chem. Eng. Sci. 54* (1999) p. 5071.
[23] Sokolichin, A.; Eigenberger, G., *Chem. Eng. Sci. 49* (1994) p. 5735.
[24] Sokolichin, A.; Eigenberger, G., *Chem. Eng. Sci. 54* (1999) p. 2273.
[25] Clift, R.; Grace, J. R. ; Weber, M. E., *Bubbles, Drops and Particles*, Academic Press, San Diego 1978.
[26] Fan, L. S.; Tsuchiya, K., *Bubble Wake Dynamics in Liquids and Liquid-Solid Suspensions*, Butterworth-Heinemann, Boston 1990.
[27] Mendelson, H. D., *AIChE J. 13* (1967) p. 250.
[28] Harmathy, T. J., *AIChE J. 6* (1960) p. 281.
[29] Rhie, C. M.; Chow, W. L., *AIAA J. 21* (1983) p. 1525.
[30] Van Doormal, J.; Raithby, G. D., *Numer. Heat Transf. 7* (1984) p. 147.

